

**Doping and disorder in the  $\text{Co}_2\text{MnAl}$  and  $\text{Co}_2\text{MnGa}$  half-metallic Heusler alloys**K. Özdoğan,<sup>1,\*</sup> E. Şaşıoğlu,<sup>2,3,†</sup> B. Aktaş,<sup>1</sup> and I. Galanakis<sup>4,‡</sup><sup>1</sup>*Department of Physics, Gebze Institute of Technology, Gebze, 41400, Kocaeli, Turkey*<sup>2</sup>*Institut für Festkörperforschung, Forschungszentrum Jülich, D-52425 Jülich, Germany*<sup>3</sup>*Fatih University, Physics Department, 34500, Büyükkçekmece, İstanbul, Turkey*<sup>4</sup>*Department of Materials Science, School of Natural Sciences, University of Patras, GR-26504 Patra, Greece*

(Received 26 July 2006; revised manuscript received 8 September 2006; published 22 November 2006)

We expand our study of the full-Heusler compounds [I. Galanakis *et al.*, Appl. Phys. Lett. **89**, 042502 (2006)] to cover also the case of doping and disorder in the case of  $\text{Co}_2\text{MnAl}$  and  $\text{Co}_2\text{MnGa}$  half-metallic Heusler alloys. These alloys present a region of very small minority density of states instead of a real gap. Electronic structure calculations reveal that doping with Fe and Cr in the case of  $\text{Co}_2\text{MnAl}$  retains half-metallicity contrary to the  $\text{Co}_2\text{MnGa}$  compound. Cr impurities present an unusual behavior, and the spin moment of the Cr impurity scales almost linearly with the concentration of Cr atoms contrary to  $\text{Co}_2\text{MnZ}$  ( $Z=\text{Si, Ge, Sn}$ ) where it was almost constant. Half-metallicity is no longer preserved for both  $\text{Co}_2\text{MnAl}$  and  $\text{Co}_2\text{MnGa}$  alloys when disorder occurs and there is an excess of either Mn or *sp* atoms.

DOI: [10.1103/PhysRevB.74.172412](https://doi.org/10.1103/PhysRevB.74.172412)

PACS number(s): 75.47.Np, 75.50.Cc, 75.30.Et

Research on half-metallic ferromagnets is rapidly growing since its prediction for  $\text{NiMnSb}$  in 1983 by de Groot and his collaborators.<sup>1</sup> The driving force of interest in these materials is their potential applications in magnetoelectronics.<sup>2–6</sup> Electronic structure calculations have played a central role in the study of these materials. Several new half-metallic ferromagnetic materials and their properties have been initially predicted by theoretical *ab initio* calculations and later verified by experiments. Among the half-metallic materials, intermetallic Heusler alloys have attracted considerable attention due to their easy growth and high Curie temperatures.<sup>7,8</sup>

The full-Heusler compounds containing Co and Mn are of particular interest for spintronics since they combine high Curie temperatures and coherent growth on top of semiconductors (they consist of four fcc sublattices with each one occupied by a single chemical element). The electronic and magnetic properties of the perfectly ordered compounds have been extensively discussed in Ref. 7. To precisely control the properties of these compounds we have to study effects susceptible of inducing states within the minority-spin gap and thus destroy the half-metallicity. States at the interfaces of these compounds with semiconductors<sup>9</sup> as well as temperature-driven excitations<sup>10–12</sup> seem to destroy half-metallicity. In addition to interface states and temperature, the third main effect which can destroy half-metallicity is the appearance of defects and disorder.<sup>13</sup>

In a recent paper<sup>14</sup> we studied the effect of doping and disorder on the magnetic properties of the  $\text{Co}_2\text{MnSi}$ ,  $\text{Co}_2\text{MnGe}$ , and  $\text{Co}_2\text{MnSn}$  full-Heusler alloys. Doping simulated by the substitution of Cr and Fe for Mn in these alloys overall keeps the half-metallicity. The effect of doping depended clearly on the position of the Fermi level, having the largest one in the case of  $\text{Co}_2\text{MnSi}$  where the Fermi level is near the edge of the minority-spin gap. On the other hand, disorder, simulated either by excess of Mn atoms at the *D* site occupied in the perfect compound by the *sp* atoms or vice versa, was found to be more important for heavy *sp* atoms like Sn but in general half-metallicity was almost preserved (see Fig. 1 in Ref. 8 for the lattice structure).

In this paper we expand our theoretical work to include also the case of  $\text{Co}_2\text{MnAl}$  and  $\text{Co}_2\text{MnGa}$  compounds which

have one valence electron fewer than that of the previous ones. Doping by electrons simulated by partial substitution of Fe for Mn in the unit cell has little effect on the gap properties while Cr impurities, corresponding to hole doping, exhibit a more unusual behavior. A high degree of spin polarization at the Fermi level is overall preserved, but contrary to what happens for the Si, Ge, and Sn compounds and to the Fe-doping case, Cr impurities present a very small spin moment for small concentrations which increases with the concentration. In the last part of our study we concentrate on the case of disorder which is shown to severely affect half-metallicity contrary to the  $\text{Co}_2\text{MnZ}$  ( $Z=\text{Si, Ge, Sn}$ ) alloys. The electronic structure calculations are performed using the full-potential nonorthogonal local-orbital minimum-basis band structure scheme (FPLO).<sup>15</sup> Finally we should note that we discuss half-metallicity in terms of total spin moments since perfect half-metals show Slater-Pauling behavior.<sup>7</sup> Spin polarization at the Fermi level is not considered since it remains very close to a perfect 100% upon doping and its exact value depends on computational details contrary to the total spin moments which were found to be more robust.

Before presenting our results we have drawn in Fig. 1 the atom-resolved density of states (DOS) for the  $\text{Co}_2\text{MnZ}$  compounds. In the left column are the case with *Z* a *sp* element belonging to the IIIB column of the periodic table (Al and Ga) and in the right column the case of IVB elements (Si, Ge, and Sn). The extra electron in the latter case occupies majority states leading to an increase of the exchange splitting between the occupied majority and unoccupied minority states and thus to larger gap width for the Si-, Ge-, and Sn-based compounds. In the case of Al- and Ga-based alloys the bonding and antibonding minority *d* hybrids almost overlap and the gap is substituted by a region of very small minority DOS; we will call it a pseudogap. In all cases the Fermi level falls within the gap or the pseudogap and an almost perfect spin-polarization at the Fermi level is preserved.

First, we will study the doping in these compounds. We substitute either Fe or Cr for Mn to simulate the doping by electrons and holes, respectively. We study the cases of moderate doping by substituting 5%, 10%, and 20% of the Mn

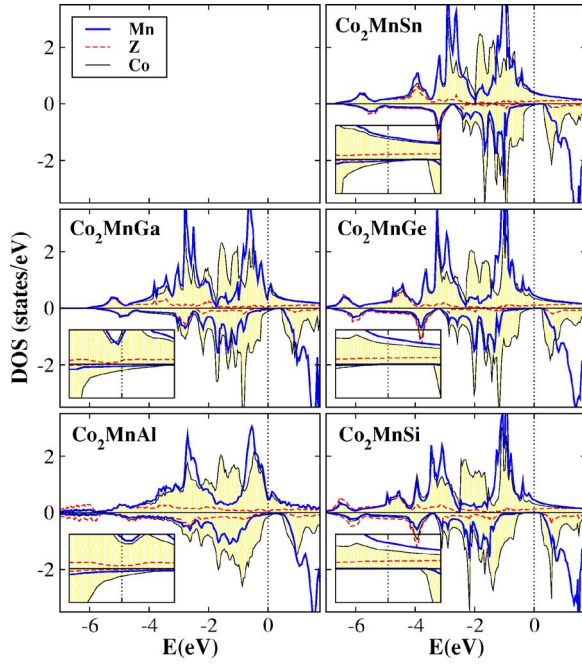


FIG. 1. (Color online) Atom-resolved density of states (DOS) for the  $\text{Co}_2\text{MnZ}$  compounds, where Z is Al, Ga, Si, Ge, and Sn. We have set the Fermi level as the zero of the energy axis. In the insets we have blown up the region around the Fermi level. Note that positive values of the DOS refer to the majority-spin electrons and negative values to the minority-spin electrons.

atoms. In our calculations the use of a coherent potential approximation ensures doping in a random way. In Fig. 2 we present the total DOS for the  $\text{Co}_2\text{Mn}_{1-x}(\text{Fe or Cr})_x\text{Al}$  alloys to compare to the perfect  $\text{Co}_2\text{MnAl}$  alloys, and in Table I we have gathered the total and atom-resolved spin moments for both Al- and Ga-based alloys. Note that in the figure we have blown up in the insets the region around the Fermi level where the gap exists.

Figure 2 confirms the discussion in Ref. 7 that the gap is created between states located exclusively at the Co sites. As was the case also for the compounds in Ref. 14 the majority-spin occupied states form a common Mn-Co band while the

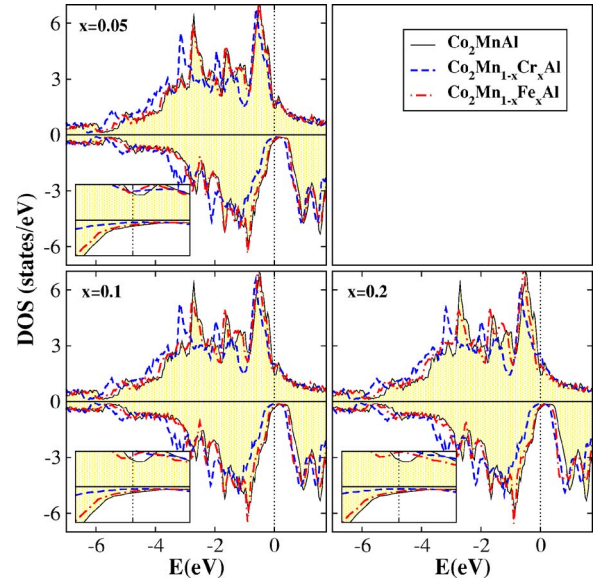


FIG. 2. (Color online) Spin-resolved DOS for the case of  $\text{Co}_2\text{Mn}_{1-x}\text{Cr}_x\text{Al}$  and  $\text{Co}_2\text{Mn}_{1-x}\text{Fe}_x\text{Al}$  for three values of the doping concentration  $x$ . DOS are compared to the one of the undoped  $\text{Co}_2\text{MnAl}$  alloys. Details as in Fig. 1.

occupied minority states are mainly located at the Co sites and minority unoccupied at the Mn sites (note that the minority unoccupied states near the gap are Co like but overall the Mn weight is dominant). Doping the perfect ordered alloy with Fe has only a marginal effect on the total DOS compared to the more significant effects of the doping with Cr. In the latter case it seems that Cr doping slightly opens the pseudogap and pushes both the majority and minority occupied bands lower in energy. This behavior upon Cr doping is also reflected on the spin moment of the Cr impurity atoms as we will discuss later in the paper and is in contrast to what happens upon Cr doping for the  $\text{Co}_2\text{MnSi}$  compound presented in Ref. 14 where the DOS scarcely changed. The important detail is what happens around the Fermi level and to what extent the gap in the minority band is affected by the doping. So now we will concentrate only on the enlarged regions around the Fermi level. The blue dashed lines repre-

TABLE I. Total and atom-resolved spin magnetic moments for the case of Fe and Cr doping of the Mn site in  $\mu_B$ . The total moment in the cell is the sum of the atomic ones multiplied by the concentration of this chemical element. Note that for Cr, Mn, and Fe we have scaled the spin moments to one atom and that for Co we give the sum of the moments of both atoms.

	Total	Co	Mn	Cr	$sp$	Total	Co	Mn	Fe	$sp$	Total	Co	Mn	Cr	$sp$	Total	Co	Mn	Fe	$sp$	
$x$	$\text{Co}_2\text{Mn}_{1-x}\text{Cr}_x\text{Al}$					$\text{Co}_2\text{Mn}_{1-x}\text{Fe}_x\text{Al}$					$x$	$\text{Co}_2\text{Mn}_{1-x}\text{Cr}_x\text{Si}$					$\text{Co}_2\text{Mn}_{1-x}\text{Fe}_x\text{Si}$				
0.00	4.04	1.36	2.82		-0.14	4.04	1.36	2.82		-0.14	0.00	5.00	1.96	3.13		-0.09	5.00	1.96	3.13		-0.09
0.05	3.95	1.49	2.69	0.34	-0.13	4.06	1.44	2.76	2.78	-0.13	0.05	4.95	1.97	3.12	2.06	-0.09	5.05	2.02	3.13	2.87	-0.09
0.10	3.90	1.51	2.71	0.62	-0.11	4.11	1.49	2.76	2.78	-0.13	0.10	4.90	1.97	3.12	2.07	-0.09	5.09	2.06	3.17	2.85	-0.08
0.20	3.80	1.54	2.74	0.91	-0.11	4.21	1.58	2.76	2.79	-0.13	0.20	4.80	1.97	3.12	2.09	-0.08	5.14	2.13	3.16	2.82	-0.08
$x$	$\text{Co}_2\text{Mn}_{1-x}\text{Cr}_x\text{Ga}$					$\text{Co}_2\text{Mn}_{1-x}\text{Fe}_x\text{Ga}$					$x$	$\text{Co}_2\text{Mn}_{1-x}\text{Cr}_x\text{Ge}$					$\text{Co}_2\text{Mn}_{1-x}\text{Fe}_x\text{Ge}$				
0.00	4.09	1.30	2.88		-0.10	4.09	1.30	2.88		-0.10	0.00	5.00	1.87	3.20		-0.06	5.00	1.87	3.20		-0.06
0.05	4.05	1.36	2.93	0.20	-0.10	4.15	1.36	2.90	2.76	-0.10	0.05	4.95	1.86	3.21	2.05	-0.06	5.05	1.91	3.22	2.88	-0.06
0.10	4.00	1.39	2.94	0.55	-0.10	4.20	1.41	2.90	2.76	-0.10	0.10	4.90	1.86	3.22	2.07	-0.06	5.10	1.96	3.23	2.88	-0.06
0.20	3.88	1.42	2.97	0.91	-0.09	4.30	1.52	2.92	2.77	-0.10	0.20	4.80	1.86	3.22	2.10	-0.06	5.19	2.06	3.26	2.89	-0.05

TABLE II. Total and atom-resolved spin magnetic moments for the case of Cr doping of the Mn site for both Al- and Si-based compounds in  $\mu_B$ . Details as in Table I.

$x$	$\text{Co}_2\text{Mn}_{1-x}\text{Cr}_x\text{Al}$					$\text{Co}_2\text{Mn}_{1-x}\text{Cr}_x\text{Si}$				
	Total	Co	Mn	Cr	$sp$	Total	Co	Mn	Cr	$sp$
0.00	4.04	1.36	2.82		-0.14	5.00	1.96	3.13		-0.09
0.20	3.80	1.54	2.74	0.91	-0.11	4.80	1.97	3.12	2.09	-0.08
0.40	3.60	1.55	2.77	1.20	-0.10	4.60	1.95	3.12	2.12	-0.08
0.60	3.40	1.54	2.79	1.37	-0.09	4.40	1.93	3.13	2.15	-0.07
0.80	3.20	1.53	2.83	1.48	-0.08	4.20	1.91	3.13	2.17	-0.07
1.00	3.00	1.46		1.63	-0.09	4.00	1.89		2.17	-0.06

sent the Cr doping while the red dash-dotted lines are the Fe-doped alloys. The situation is reversed with respect to the  $\text{Co}_2\text{MnSi}$  compound; Cr doping has significant effects on the pseudogap. Its width is larger with respect to the perfect compound and becomes slightly narrower as the degree of the doping increases. We will discuss this behavior in detail later in the text. Fe doping, on the other hand, almost does not change the DOS around the Fermi level. The extra electrons occupy high-energy lying antibonding majority states, but since  $\text{Co}_2\text{MnAl}$  has one valence electron fewer than  $\text{Co}_2\text{MnSi}$ , half-metallicity remains energetically favorable and no important changes occur upon Fe doping and further substitution of Fe for Mn should retain the half-metallicity even for the  $\text{Co}_2\text{FeAl}$  compound. In reality  $\text{Co}_2\text{FeAl}$  is almost half-metallic as discussed in Ref. 16.

In Table I we have gathered the spin magnetic moments for all cases under study. For perfect half-metals the total spin moment  $M_t$  follows Slater-Pauling (SP) behavior, being the number of the valence electrons in the unit cell minus 24.<sup>7</sup> The perfect  $\text{Co}_2\text{MnAl}$  and  $\text{Co}_2\text{MnGa}$  compounds have total spin moments slightly larger than the ideal  $4\mu_B$  predicted by the SP rule while the total spin moments of the Si- and Ge-based alloys are exactly  $5\mu_B$  as predicted by the SP rule. In the case of the chemically disordered compounds, doping by 5%, 10%, or 20% of Cr (or Fe) atoms means that the mean value of the total number of valence electrons in the unit cell is decreased (or increased, respectively) by 0.05, 0.10, and 0.20 electrons, respectively. Half-metallicity is retained only when we dope  $\text{Co}_2\text{MnAl}$ . On the other hand, for the  $\text{Co}_2\text{MnGa}$  compound the Fermi level is deeper in energy as shown in Fig. 1 and both perfect and disordered compounds are not half-metallic.

The atom-resolved spin moments in Table I present a striking peculiarity when we dope with Cr. In the case of  $\text{Co}_2\text{MnSi}$  (or Ge) compounds, the Cr impurities have a moment of slightly larger than  $2\mu_B$ , independent of the degree of doping. Similarly Fe impurities have a spin moment of around  $2.8\mu_B$ . In the case of the  $\text{Co}_2\text{MnAl}$  and  $\text{Co}_2\text{MnGa}$  compounds Fe impurities also have a large spin moment of the same order of magnitude. But Cr impurities have a very small spin moment ( $0.3\mu_B$  for the Al compounds and  $0.2\mu_B$  for the Ga compound) for the case of 5% doping. Substituting 10% or 20% of Cr for the Mn atoms leads to a doubling or tripling, respectively, of the Cr-impurity spin moment. To elucidate this behavior, we have performed calculations for

both  $\text{Co}_2[\text{Mn}_{1-x}\text{Cr}_x]\text{Al}$  and  $\text{Co}_2[\text{Mn}_{1-x}\text{Cr}_x]\text{Si}$  compounds for values of  $x$  ranging from 0 to 1 and we have gathered the atom-resolved spin moment in Table II and in Fig. 3 we have drawn the Cr-resolved DOS for three values of  $x$ . In the case of Si compounds the Cr-impurity spin moment is almost constant irrespective of the concentration. On the other hand, for the Al compounds the spin moment of the Cr impurities increases with the concentration of Cr atoms. Figure 3 explains this phenomenon. In the case of Si compounds the Fermi level falls after the majority peak and upon doping the relative position of the Fermi level does not change. This peak comes from the  $d$  electrons of Cr and can be decomposed in (i) a very localized in energy and high-intensity peak coming from the double degenerated  $e_g$  electrons (the Fermi level is pinned with respect to this peak) and (ii) a more broad and lower-intensity peak due to the triple-degenerated  $t_{2g}$   $d$  electrons; in the case of the Al compounds, as we dope them, we change slightly the Coulomb repulsion and the exchange splitting and these  $t_{2g}$  electrons move lower in energy with respect to the  $e_g$  ones and, consequently, the Fermi level, creating also the shoulder presented for  $x=0.8$  and reducing the Cr atomic spin moment. We should also note that the Fermi level falls within a maximum of the Cr-resolved DOS,

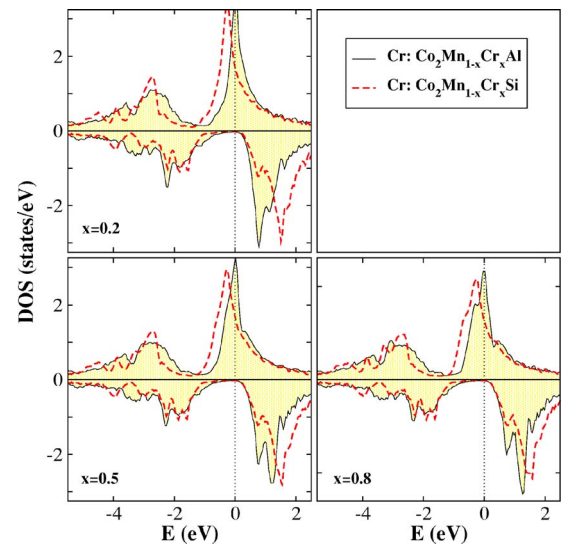


FIG. 3. (Color online) Cr-resolved DOS in the case of the  $\text{Co}_2\text{Mn}_{1-x}\text{Cr}_x\text{Al}$  and  $\text{Co}_2\text{Mn}_{1-x}\text{Cr}_x\text{Si}$  compounds for three different values of the concentration  $x$ . Details as in Fig. 1.



TABLE III. Total and atom-resolved spin magnetic moments for the case of excess of Mn ( $x$  positive) or  $sp$  atoms ( $x$  negative) atoms. In the second column the ideal total spin moment if the compound was half-metallic. Details as in Table I.

$x$	$\text{Co}_2\text{Mn}_{1+x}\text{Al}_{1-x}$					$\text{Co}_2\text{Mn}_{1+x}\text{Ga}_{1-x}$			
	Ideal	Total	Co	Mn	Al	Total	Co	Mn	Ga
-0.20	3.40	3.26	1.09	2.89	-0.12	3.40	1.11	3.00	-0.09
-0.10	3.70	3.64	1.22	2.84	-0.13	3.74	1.21	2.94	-0.10
-0.05	3.85	3.83	1.29	2.83	-0.13	3.92	1.25	2.93	-0.10
0.00	4.00	4.04	1.36	2.82	-0.14	4.09	1.31	2.88	-0.10
0.05	4.15	4.22	1.40	2.81	-0.14	4.29	1.36	2.89	-0.11
0.10	4.30	4.40	1.44	2.81	-0.14	4.48	1.40	2.88	-0.11
0.20	4.60	4.80	1.54	2.81	-0.15	4.85	1.50	2.87	-0.11

but as shown clearly in Fig. 2 this is only a local maximum and thus we do not expect it to seriously affect the stability of the lattice structure.

In the last part of our study we study the effect of disorder. We either create an excess of the Mn or the  $sp$  atoms. In Table III we have gathered the total and atomic spin moments for all cases under study. Substituting 5%, 10%, 15%, or 20% of the Mn atoms by the Al or Ga ones, corresponding to the negative values of  $x$  in the table, results in a decrease of 0.15, 0.30, 0.45, and 0.60 of the total number of valence electrons in the cell, while the inverse procedure results in a similar increase of the mean value of the number of valence electrons. Contrary to the Si, Ge, and Sn compounds presented in Ref. 14 which retained perfect half-metallicity, the Al- and Ga-based compounds are no longer half-metallic. In the case of the Si and related compounds disorder-induced states at the edges of the gap keep the half-metallic character

but this is no longer the case for the Al and Ga compounds where no real gap exists.

We have studied the effect of doping and disorder on the magnetic properties of the  $\text{Co}_2\text{MnAl}$  and  $\text{Co}_2\text{MnGa}$  full-Heusler alloys. These compounds present a region of a low minority density of states instead of a real gap. Doping simulated by the substitution of Cr and Fe for Mn overall keeps half-metallicity for  $\text{Co}_2\text{MnAl}$  while the Ga compounds present deviations. The spin moment of the Cr impurities varies considerably with the concentration, and this behavior is attributed to the position of the majority  $t_{2g}$   $d$  electrons with respect to the majority  $e_g$  electrons. Disorder simulated by excess of either Mn or  $sp$  atoms completely destroys the almost perfect spin polarization of the perfect compounds. It seems that  $\text{Co}_2\text{MnAl}$  and  $\text{Co}_2\text{MnGa}$  compounds are less adequate than the  $\text{Co}_2\text{MnSi}$ ,  $\text{Co}_2\text{MnGe}$ , and  $\text{Co}_2\text{MnSn}$  alloys for realistic spintronic applications.

\*Electronic address: kozdogan@gyte.edu.tr

†Electronic address: e.sasioglu@fz-juelich.de

‡Electronic address: galanakis@upatras.gr

<sup>1</sup>R. A. de Groot, F. M. Mueller, P. G. van Engen, and K. H. J. Buschow, Phys. Rev. Lett. **50**, 2024 (1983).

<sup>2</sup>*Half-Metallic Alloys: Fundamentals and Applications*, edited by I. Galanakis and P. H. Dederichs, *Lecture Notes in Physics*, Vol. 676 (Springer, Berlin, 2005).

<sup>3</sup>A. Bergmann, J. Grabis, B. P. Toperverg, V. Leiner, M. Wolff, H. Zabel, and K. Westerholt, Phys. Rev. B **72**, 214403 (2005); J. Grabis, A. Bergmann, A. Nefedov, K. Westerholt, and H. Zabel, *ibid.* **72**, 024437 (2005); **72**, 024438 (2005).

<sup>4</sup>S. Kämmerer, A. Thomas, A. Hütten, and G. Reiss, Appl. Phys. Lett. **85**, 79 (2004); J. Schmalhorst, S. Kämmerer, M. Sacher, G. Reiss, A. Hütten, and A. Scholl, Phys. Rev. B **70**, 024426 (2004).

<sup>5</sup>Y. Sakuraba, J. Nakata, M. Oogane, H. Kubota, Y. Ando, A. Sakuma, and T. Miyazaki, Jpn. J. Appl. Phys., Part 2 **44**, L1100 (2005).

<sup>6</sup>X. Y. Dong, C. Adelman, J. Q. Xie, C. J. Palmström, X. Lou, J. Strand, P. A. Crowell, J.-P. Barnes, and A. K. Petford-Long, Appl. Phys. Lett. **86**, 102107 (2005).

<sup>7</sup>I. Galanakis, Ph. Mavropoulos, and P. H. Dederichs, J. Phys. D **39**, 765 (2006); I. Galanakis, P. H. Dederichs, and N. Papani-

kolaou, Phys. Rev. B **66**, 174429 (2002).

<sup>8</sup>E. Şaşıoğlu, L. M. Sandratskii, P. Bruno, and I. Galanakis, Phys. Rev. B **72**, 184415 (2005).

<sup>9</sup>J. J. Attema, G. A. de Wijs, and R. A. de Groot, J. Phys. D **39**, 793 (2006); K. Nagao, Y. Miura, and M. Shirai, Phys. Rev. B **73**, 104447 (2006); I. Galanakis, M. Ležaić, G. Bihlmayer, and S. Blügel, *ibid.* **71**, 214431 (2005); I. Galanakis, J. Phys.: Condens. Matter **16**, 8007 (2004).

<sup>10</sup>L. Chioncel, E. Arrigoni, M. I. Katsnelson, and A. I. Lichtenstein, Phys. Rev. Lett. **96**, 137203 (2006); L. Chioncel, M. I. Katsnelson, R. A. de Groot, and A. I. Lichtenstein, Phys. Rev. B **68**, 144425 (2003).

<sup>11</sup>M. Ležaić, Ph. Mavropoulos, J. Enkovaara, G. Bihlmayer, and S. Blügel, Phys. Rev. Lett. **97**, 026404 (2006).

<sup>12</sup>R. Skomski and P. A. Dowben, Europhys. Lett. **58**, 544 (2002).

<sup>13</sup>J. J. Attema, C. M. Fang, L. Chioncel, G. A. de Wijs, A. I. Lichtenstein, and R. A. de Groot, J. Phys.: Condens. Matter **16**, S5517 (2004).

<sup>14</sup>I. Galanakis, K. Özdoğan, B. Aktaş, and E. Şaşıoğlu, Appl. Phys. Lett. **89**, 042502 (2006).

<sup>15</sup>K. Koepernik and H. Eschrig, Phys. Rev. B **59**, 1743 (1999); K. Koepernik, B. Velicky, R. Hayn, and H. Eschrig, *ibid.* **58**, 6944 (1998).

<sup>16</sup>I. Galanakis, J. Phys.: Condens. Matter **16**, 3089 (2004).